Environmental
Science
Water Research & Technology

Bioaccumulation of silver nanoparticles in model wastewater biofilms

Journal:	*Environmental Science: Water Research & Technology*
Manuscript ID	EW-ART-02-2018-000102.R1
Article Type:	Paper
Date Submitted by the Author:	07-May-2018
Complete List of Authors:	Walden, Connie; University of Arkansas, Civil Engineering Zhang, Wen; University of Arkansas, Civil Engineering

SCHOLARONE™
Manuscripts

Water Impact Statement

Engineered nanoparticles are increasingly incorporated into consumer products and inevitably released into wastewater. This work investigated if wastewater biofilm can successfully remove silver nanoparticles. The phenomena of nanoparticle accumulation within the biofilm and their subsequent release could also be applied to other applications involving nanoparticle – biofilm interactions.

Environmental Science: Water Research & Technology

ARTICLE

Bioaccumulation of silver nanoparticles in model wastewater biofilms

C. Walden,[a] W. Zhang[b]

Engineered nanoparticles are increasingly incorporated into consumer products and inevitably released into wastewater. This study explored the capacity for wastewater biofilm to accumulate and release silver nanoparticles (Ag-NPs). Synthetic wastewater (SW) was used to feed wastewater biofilm in two types of reactors: a CDC biofilm reactor (CBR) and a flow cell. Using typical wastewater bacteria (*Acinetobacter calcoaceticus, Comamonas testosteroni,* and *Delftia acidovorans*) as a model consortium, biofilm functionality, structure, and viability were monitored with and without Ag-NPs exposure in CBR. At a design concentration of 200 ppb, no significant change in biofilm viability or functionality were observed. However, significant cell stress was detected with the generation of excess reactive oxygen species. To measure Ag-NP accumulation, the flow cell experiments were performed for each species singly, in dual combinations, and mixed at the same design concentration as previous. The single species biofilms accumulated the least amount of silver, approximately 0.01 ng mm^{-2}. The dual species, *A. calcoaceticus* and *D. acidovorans* accumulated 0.43 ng mm^{-2}, the highest measured concentration of these combinations. This combination was then further tested for the possible release of silver. After Ag-NP exposure, biofilm detachment and total silver concentrations in influent and effluent were measured. While effluent cell counts did not significantly change (p>0.05), the measured silver attached to the biofilm significantly decreased (p=0.04). This shows that small concentrations of silver attached to the biofilm and was subsequently released. Given the dynamic nature of living biofilms, this study indicates that wastewater biofilm plays a small role in silver transport in wastewater networks. Further, this work could potentially apply to the fundamental understanding of biofilm – NP interactions in other systems.

Introduction

Anthropogenic influences can negatively impact long-term water quality of community water resources (*i.e.* reservoirs) that serve for drinking water and recreation. When wastewater treatment plants can no longer accommodate the needs of a growing community while still maintaining environmental discharge limits, engineers are tasked with designing processes that can meet current and future wastewater discharge requirements, while minimizing the plant footprint and operating costs. Although activated sludge processes remained the popular choice in the United States since the 1970s, scientific advances have afforded engineers more options such as biofilters, tertiary membrane filtration, and enhanced phosphorus removal. A more reasonable choice, communities opt to upgrade an existing plant when possible, as opposed to building a new plant. For example, the city of Folkston, Georgia added a moving bed biofilm reactor (MBBR) into existing activated sludge tanks for increased nutrient removal capacity without adding to the plant footprint.[1] Further examples include the addition of integrated fixed film activated sludge (IFAS) processes to existing plants in locations such as Neptune Beach, FL and Narragansett Bay, RI.[2] These are just a few examples of the ways biofilm processes are incorporated into existing structures to enhance wastewater treatment plants. These upgrades utilizing biofilm processes can improve treatment capacity by as much as 200% while maintaining the same land footprint.

Biofilms are ubiquitous in aquatic environments such as piping systems and surface waters when microorganisms attach to a surface and exude extracellular polymeric substances (EPS).[3] The EPS matrix includes a heterogeneous mixture of proteins, polysaccharides, phospholipids, and nucleic acids that protect the cells from possible stressors.[4] As plant upgrades are meant for improving treatment capacity and nutrient removal, it is important to understand the interaction between biofilms and a variety of possible contaminants. The addition of engineered nanoparticles (ENPs) in consumer products has opened the opportunity for research on the transport and accumulation of ENPs in the environment.[5] Without effective treatment and source water protection, the presence of ENPs and subsequent release into the ecosystem can result in bioaccumulation in crops and aquatic species, which could have implications in food web transfer. We have already seen that the partitioning of ENPs is influenced by the presence of biofilms.[6] Studies on biofilm-ENP interactions in wastewater treatment plants have mainly focused on toxicity and inhibitory effects on biofilm

[a] *Graduate Assistant. Department of Civil Engineering, University of Arkansas, Fayetteville, Arkansas 72712.*
[b] *Assistant Professor. Department of Civil Engineering, University of Arkansas, Fayetteville, Arkansas 72712.*

† Footnotes. None.
Electronic Supplementary Information (ESI) available: None.

This journal is © The Royal Society of Chemistry 2018

Environ. Sci.: Water Research & Tech., 2018, **00**, 1-3 | **1**

formation.[7-9] Results continually agree that biofilms are more resistant to greater levels of nanoparticles than planktonic bacteria, as EPS provides a protective barrier for bacteria cells.[10-12] Yet, the capacity for biofilm to accumulate ENPs has not been well studied. Structural thinning was observed with single species biofilm after exposure to multiple concentrations of silver nanoparticles (Ag-NPs) (0 – 2000 ppb), while no change in viability was observed in *Pseudomonas putida* among concentrations of Ag-NPs or pH values.[13] In contrast, *Aquabacterium citratiphilum* (a model for freshwater biofilm) showed no significant change in biofilm thickness when exposed to Ag-NPs (0 – 2400 ppb).[14]

Simple, one species models are regularly sufficient for examination of biofilm systems when evaluating antimicrobial activity, toxicity tests, or antibiofilm products. Here, we developed a mixed species wastewater biofilm as a model to further assess the capacity for wastewater biofilms to accumulate ENPs. The model biofilm, comprised of three representative species found in wastewater, was first tested for reproducibility and similarity to wastewater biofilms by considering the biofilm formation capacity of each species alone and in combinations in synthetic wastewaters. Then, the impact of ENPs on model biofilm functionality was compared to previously observed biofilm functions in the presence of ENPs. After establishing the reliability of the laboratory model, the biofilm was tested individually and in multiple combinations to quantify ENP accumulation. We also considered the possibility of re-release after ENP attachment. Ag-NPs, a common ENP in food packaging, drug delivery, and textiles, were used as a model ENP.

Materials and Methods

Chemicals. Glassware used for nanoparticle synthesis was acid washed in 10% hydrochloric acid, rinsed three times with distilled deionized (DDI) water and air dried [Elga Process Water System (18.2 MΩ · cm^{-1}) Purelab flex, Veolia, Ireland]. All laboratory glassware was cleaned in phosphorous-free detergent, rinsed three times with tap water, and three times with DDI prior to additional cleaning procedures.

Analytical grade reagents were stored as directed and used as received. Synthetic wastewater (SW) was chosen by comparing three recipes, listed as referenced.[15-17] The SW chosen as feed solution was prepared with glucose (140 mg L^{-1}), Difco nutrient broth (300 mg L^{-1}), KH_2PO_4 (43.9 mg L^{-1}), NaOH (25 mg L^{-1}), KNO_3 (3 mg L^{-1}), $NaHCO_3$ (175 mg L^{-1}), $(NH_4)_2SO_4$ (118 mg L^{-1}), $CaCl_2$ (133 mg L^{-1}), $FeCl_3·6H_2O$ (5 mg L^{-1}), $MgSO_4$ (100 mg L^{-1}), and $MnSO_4$ (12.8 mg L^{-1}).[16] Orthophosphate, nitrate, sulfate, chloride ions were measured with Ion Chromatography (Metrohm 850 IC, Switzerland). Ammonia was measured by salicylate method on a spectrophotometer (AmVer 3 Hach reagent kit, Hach, Loveland, CA). Chemical Oxygen Demand (COD) was measured in triplicate on a COD block heater with a new blank for each measurement (Hach, Loveland, CA).

Microbial culture. The strains *Comamonas testosteroni* ATCC 11996, *Acinetobacter calcoaceticus* ATCC 31926 and *Delftia acidovorans* ATCC 15668 were obtained and propagated as

instructed in Difco nutrient broth at 30°C for 48 hours. Cultures were propagated on agar plates and stored for no longer than 30-day increments at 4°C. Visual monitoring ensured that compromised agar plates were disposed of. Cell counts in liquid culture were measured in triplicate with a Multisizer 4 Coulter Counter (Beckman Coulter, CA, USA). Prior to the experiment, one colony of each species was inoculated and grown in 50 mL of SW until reaching an optical density of approximately 0.1 on a spectrophotometer at 620 nm (Beckman Coulter DU720 UV/VIS Spectrophotometer, Beckman Coulter Inc., Brea, CA).

Biofilm formation assay. A 1:100 dilution of 100 µL cell suspension in SW was transferred aseptically to a sterile microtiter 96-well plate for each species with six replicates.[18, 19] Multiple combinations between these species were tested: *A. calcoaceticus; C. testosteroni; Delftia acidovorans; A. calcoaceticus* and *C. testosteroni*; *A. calcoaceticus* and *Delftia acidovorans*: *C. testosteroni* and *Delftia acidovorans*; as well as a combination of all three together. The microtiter plate included six wells of SW without inoculation as the negative control. The plate was incubated at 37°C for 24 hours, rinsed and stained with crystal violet.[20] To quantify the biofilm, 125 µL of 30% acetic acid was added to each well and incubated for 15 minutes. Absorbance at 590 nm was recorded for each using 30% acetic acid as the blank.[19, 21] Formation is quantified by comparing the absorbance (Abs) of the inoculated cells to control cells, where biofilm adherence is categorized as the following: $Abs \leq Abs_{control}$ are considered non-adherent (0), $Abs_{control} < Abs \leq 2 \times Abs_{control}$ are weakly adherent (+), $2 \times Abs_{control} < Abs \leq 4 \times Abs_{control}$ are moderately adherent (++), and $Abs > 4 \times Abs_{control}$ are considered strongly adherent (+++).

Nanoparticle characterization. Silver nanoparticles were synthesized using sodium borohydride to reduce silver nitrate with sodium citrate as a capping agent.[22] The formation of Ag-NPs was confirmed by scanning the absorbance from 300 – 700 nm with a UV-vis spectrophotometer (Beckman Coulter, CA, USA). Size and shape were characterized with transmission and scanning electron microscopy. Total silver concentrations were prepared by Standard Method 3500-Ag and measured with ICP-MS (iCapQ Quadrupole with Cetac ASX-560 autosampler, Arkansas Mass Spec Facility). Ionic silver and nano-particulate silver were measured separately by applying multiple separation techniques. Samples for nano-particulate measurement were filtered with 0.1 µm Acrodisc syringe filters (Life Sciences, Colorado), where the total silver in the filtrate is less than 100 nm in size, was compared with the total silver concentration. 2 mL samples were also loaded in 3kDa Amicon Ultra 4 centrifugal filters (Merck Millipore, Massachusetts) where the filtrate concentration is solely ionic silver.

Experimental setup. Preceding experimentation, SW pH was measured with a pH meter and adjusted to pH=8 with 0.1 M HCl if necessary (Thermo-Scientific, Fort Collins, Colorado). All tubing and reactors were run with 10% bleach solution and allowed to sit overnight. Then, DDI water was used to rinse. Finally, the apparatus and accessories were autoclaved at 121 °C for 30 minutes (Model 522LS Gravity Steam Sterilizer, Getinge, Rochester, New York).

2 | *Environ. Sci: Water Research & Tech.*, 2012, **00**, 1-3

This journal is © The Royal Society of Chemistry 2018

ARTICLE

The CDC biofilm reactor (CBR) (Biosurface Technologies, Bozeman, MT) was used to explore biofilm functionality and structure under dynamic conditions. The reactor is a 1-liter glass beaker with a polyethylene lid which holds 8 polyethylene rods, each with three removable polyethylene coupons serving as an attachment site for biofilm growth. The CBR operates as a continuous flow stirred tank reactor (CFSTR), where nutrients are continuously pumped in, and effluent flows out. This reactor setup is assumed well mixed, has a working volume of approximately 350 mL, and was operated at 2 mL min^{-1}, resulting in a retention time of 175 minutes. Prior to the CFSTR mode, the CBR setup was run in an incubation room at 28 °C on a stirring plate set to 80 rpm in batch mode for 24 hours, allowing a mature biofilm to form. One rod containing three coupons was removed and carefully stored in sterile SW at 28 °C for microscopic analysis. Then, the CBR was operated with SW containing approximately 50 ppb Ag-NPs at a flow rate of 2 mL min^{-1} for 3 hours, nearly one retention time. One rod with three coupons was removed, placed in SW without Ag-NPs to remove any unattached silver, and aseptically transferred to sterile SW in a brown HDPE bottle to minimize biofilm disturbance preceding microscopy.

A custom flow cell (Figure S1) was used to analyze silver bioaccumulation for each species individually and in combination. Before experimentation, the flow cell was cleaned and sterilized in the same manner as the CBR. The flow cell experiments were replicated until each experiment showed triplicate accumulation values with standard errors less than 20%.

Biofilm analysis. During functionality testing in the CBR, biofilm was also characterized by *bac*Light cell stain (Live/Dead *bac*Light Bacterial viability kit, Life Technologies, Grand Island, New York) using confocal laser scanning microscopy (CLSM). Images were obtained with a Nikon 90i upright CLSM using the 60× objective lens (Nikon, Melville, New York). 5 replicate image z-stacks were randomly selected and recorded from at least two different CBR coupons. Overall oxidative stress was measured with 2'-7'dichlorofluorescein diacetate (H$_2$-DCFDA) on a 96 well microplate reader (Synergy H1 Multi-Mode Microplate Reader, Biotek Instruments, Inc., Winooski, VT).[23-25] Briefly, three coupons representing 3 replicates were removed and cautiously dipped in phosphate buffered solution (PBS) to remove planktonic cells. Each coupon was placed in a sterile tube containing 2.5 mL of PBS and vortexed for 30 seconds with 0.4 µL of 5 mM H$_2$-DCFDA. 200 µL was then transferred to the 96-well microplate and incubated for 30 minutes in the dark at 37°. ROS was assessed at 495 nm of excitation wavelength, and 527 nm of emission wavelength. A standard curve was generated with hydrogen peroxide to ensure the performance of the instrument. Control wells included Ag-NPs with (H$_2$-DCFDA) to consider any quenching effects on the dye fluorescence emission.[26]

Ag-NP adsorption. Qualitative analysis of Ag-NP attachment to biofilms was completed by fluorescently labeling Ag-NPs for visualization with CLSM with biofilm samples. To label Ag-NPs, the particle labeling procedure was tested with different amounts of EDC (1-ethyl-3-(3-dimethylaminopropyl)

carbodiimide) and Sulfo-NHS (sulfo-hydroxysuccinimide) in MES sodium salt buffer as previously described.[27] The most efficient labeling occurred with 12 mg EDC, 0.72 nmol Rh123 in 200mM MES Buffer, followed by 24 hours agitation, then 24 hours of dialysis in 9:1 ethanol solution. Particles were visualized within 8 hours of the labeling procedure.

To quantitatively measure Ag-NP accumulation, three coupons were aseptically removed from either reactor after Ag-NP exposure, suspended in a sterile tube with 5 mL of nitric acid solution, and vortexed for 5 minutes. The coupons were then removed with tweezers, and the final volume was brought to 10 mL of 2.5% nitric acid for total silver concentration using ICP-MS.

Statistical analysis. Data compilation and tables were generated in Microsoft Excel (Microsoft, Redmond, WA). Measurements were performed in triplicate. Output files were graphed, and statistical analysis was completed in SigmaPlot version 12.5 from Systat Software, Inc., San Jose California USA, www.systatsoftware.com. To measure the statistical difference between populations, the student's t-test was applied to compare means. Statistic p values less than 0.05 were considered significant.

Results and Discussion

Mixed species biofilm model. The mixed species biofilm was thoughtfully conceived from previous studies of common bacteria species in wastewater. Successful isolation and identification of *Acinetobacter calcoaceticus* in hospitals, wastewater biological nutrient removal processes, and as a

Table 1. Effluent characteristics after each retention time of the CDC biofilm reactor totaling 12 hours (a) without Ag-NPs within the influent and (b) with 200 ppb Ag-NPs within the influent. All results are reported as an average of three measurements.

	Time (hr)	COD (mg O$_2$ L^{-1})	pH	Ammonia (mg L^{-1} NH$_3$-N)	Cl$^-$(mg L^{-1})	NO$_3^-$ (mg L^{-1})	PO$_4^{3}$ (mg L^{-1})$^-$	COD Percent Removed
(a)	0	274	8.6	18.5	122.7	1.4	3.2	
	3	131	7.0	18.7	92.8	0.2	5.6	52%
	6	229	6.5	18.0	75.9	0.2	2.9	16%
	9	229	6.2	23.9	70.3	0.2	1.5	16%
	12	141	6.3	18.9	66.2	0.3	1.4	48%
(b)	0	458	7.6	29.4	66.4	1.3	3.0	
	3	310	6.7	28.4	66.1	0.1	4.0	32%
	6	264	6.8	31.1	64.3	0.1	2.8	42%
	9	275	7.0	32.2	61.3	0.1	1.9	40%
	12	269	6.7	31.7	60.8	0.1	2.2	41%

dominant aerobic species within soil and water samples provides evidence that *A. calcoaceticus* is significant in NP - bacterial interactions.[28-30]

Multidrug-resistant and part of the normal human bacterial community dermally and within the respiratory tract, *A.*

This journal is © The Royal Society of Chemistry 2018

Environ. Sci.: Water Research & Tech., 2017, **00**, 1-3 | **3**

calcoaceticus has shown to be responsible for nosocomial infections since the 1970's.[31] Certain strains of *Acinetobacter spp.* also display the unique ability to generate silver and platinum nanoparticles in controlled experiments.[32, 33] The ubiquitous nature of this species along with its tolerance and ability to generate nanoparticles make this species an excellent model for examining NP – biofilm interactions.[34] *Delftia acidovorans* are strictly aerobic, non-fermentative chemoorganotrophs. *D. acidovorans* have been identified to occur in freshwater, soil, activated sludge and clinical samples.[35] *D. acidovorans* have the capacity to survive in potable water system biofilms and are a rare but possible cause of infection with intravenous drug users.[36] *Comamonas testosteroni* are highly motile and aerobic. Interest in *C. testosteroni* centers around activated sludge, heavy metal mining soil, and organic compound remediation.[37] The heavy metal resistance of this species is also of interest when examining NP – biofilm interactions. As discussed, these species individually are relevant model biofilm in wastewater, and they could help reveal the NP-biofilm interaction in a complex environment such as wastewater; further, NP interactions observed with these species separately and mixed will be applicable in environments other than wastewater, including hospitals, distribution systems, and freshwater environments.

Before investigating the NP-biofilm interactions, the biofilm formation capability of each species and their combination was studied first. The biofilm formation assay included staining of biofilm with crystal violet, followed by an absorbance measurement which correlates with the quantity of biofilm formed. We compared three SW recipes through a biofilm formation assay with each species to ensure the SW supports the growth of all species relatively evenly (Figure S2). The recipe showing the smallest error in biofilm formation for all three species within 24 hours was selected as representative of wastewater for this study.

Silver nanoparticle characteristics. The generated Ag-NPs exhibited a typical surface plasmon resonance with a UV-vis wavelength peak at 398 nm (Figure S3). Transmission electron microscopy particle size measurements of the stock solution showed the particle size diameter was 14.6±0.21 nm (Figure S4). Nano-sized and ionic silver concentrations were measured for both stock solution and SW suspensions. In the stock solution, the total silver concentration was 1.1 ppm. Stock solutions were stored in brown bottles in the dark until time for use. For quick checks, the UV-vis wavelength peak was used to verify no agglomeration occurred during storage. After dilution into SW, silver complexation occurred. ICP-MS results showed only 0.98% of total silver still existed as Ag-NPs, 1.2% was less than 100 nm as particulate or ionic silver, and the rest has formed agglomerates larger than 100 nm. TEM images of SW with Ag-NPs showed precipitates and particles in clusters (Figure S5), as expected. Previous research showed Ag-NPs undergo a chemical transformation in sewer networks with cysteine, histidine, sulfur and chlorides [38]. In this study, complexation of Ag-NPs occurred immediately after getting in contact with SW, which simulates environmental conditions that are expected to occur in wastewater sewers.
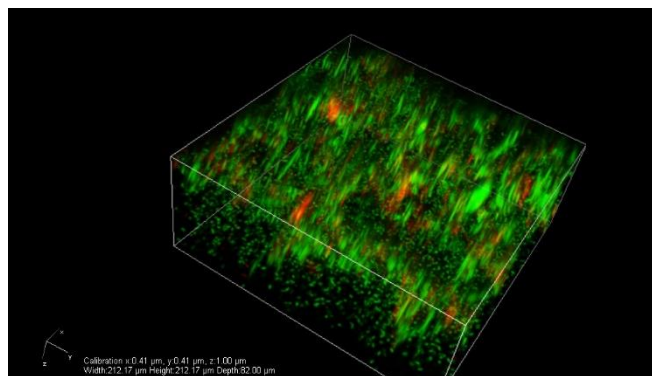

Figure 1. 3-dimensional view from confocal laser scanning microscopy for biovolume measurement of fluorescently stained model biofilm in the CBR after Ag-NP exposure. The biofilm was comprised of all three species. Green indicates live cells and red indicates damaged cells.

CBR exposure tests. A CBR was operated to assess changes in biofilm functionality in this model system during silver exposure. With all three species, the CBR was inoculated and operated in batch mode for 24 hours. After the biofilm was formed, stock Ag-NPs was added into sterile SW to a designed total silver concentration of approximately 50 ppb and pumped through the CBR at 2 mL min^{-1}. Stock dilution was performed volumetrically by pipet which incorporated small variations between experiments. Therefore measured values are reported as needed. Random influent and effluent checks of total silver ranged from 48 ppb – 67 ppb.

Biofilm structure and viability. A three-dimensional view of all intact (live) cells (green) and all damaged (dead) cells (red) shows the distribution of bacteria throughout a representative image stack (Figure 1). After 3 hours of Ag-NP exposure, live:dead ratios of biofilm formed on the coupons within the reactor were 3.66±1.01, showing no significant change in viability from live:dead ratios preceding exposure (p=0.578). This tolerance to low concentrations of Ag-NPs (at about 50 ppb) by the biofilm was expected; in fact, to achieve biofilm toxicity, concentrations were previously determined to be
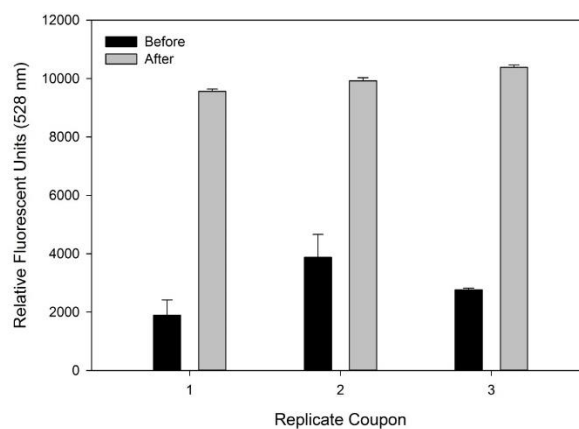

Figure 2. Reactive oxygen species detected before and after 50 ppb Ag-NP exposure to biofilms. Relative fluorescent units are after subtracting background fluorescence from the Ag-NPs.
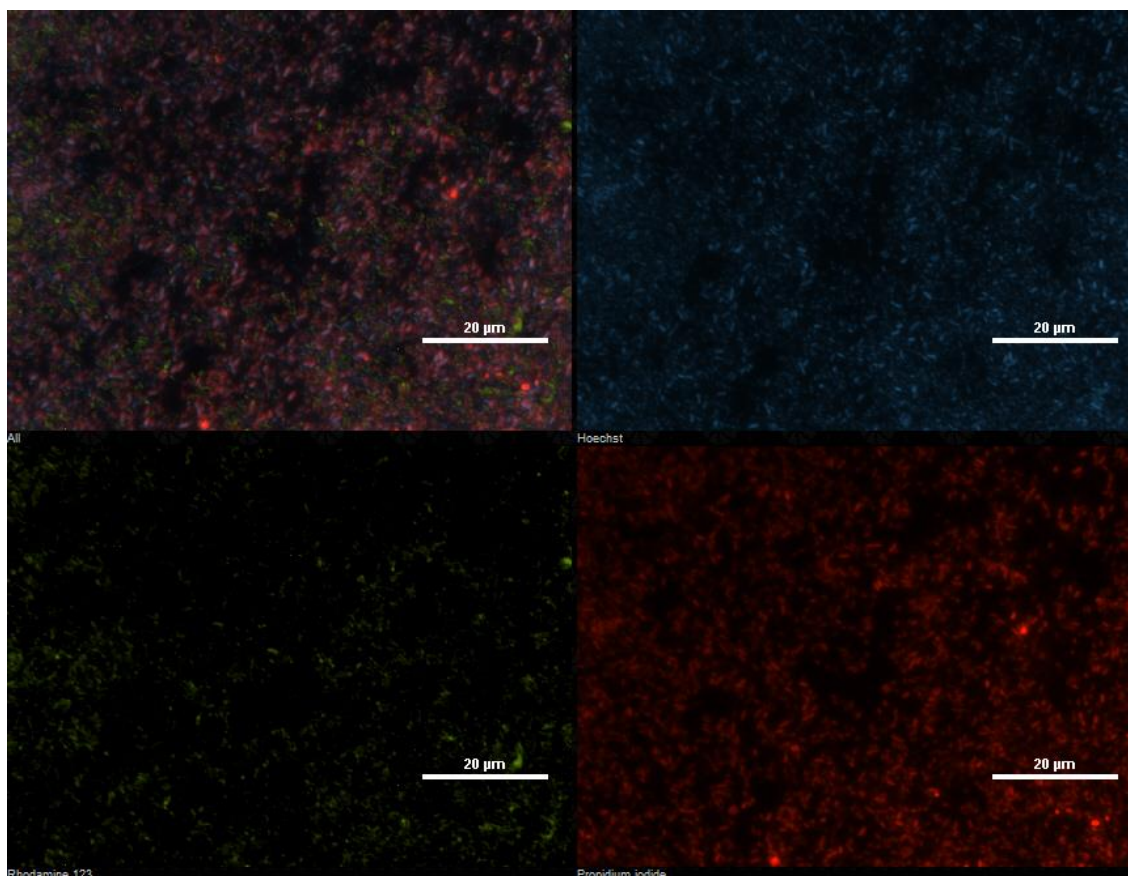
4 | *Environ. Sci: Water Research & Tech.*, 2012, **00**, 1-3

This journal is © The Royal Society of Chemistry 2018

Figure 3. Confocal laser scanning microscope image of biofilm stained with *Bac*light stains propidium iodide (red, damaged cells) and Hoescht 33358 (blue, all cells). Ag-NPs were fluorescently labeled with rhodamine123 protein (green particles) for qualitative imaging within *C. testosteroni* biofilm matrix.

higher than 5 mg L^{-1} with *Psuedomonas putida* standard toxicity tests.[39] Although toxicity will vary between species and biofilm types, the previous study corroborates that biofilm can exhibit tolerance to Ag-NPs. In our study, although viability showed no change, reactive oxygen species generated as a sign of cell stress significantly increased (p=0.006) (Figure 2).

A biovolume was also calculated in terms of fluorescent intensity using CLSM. Biovolume is a common structural parameter used in CLSM studies. Biovolume measurements were produced from the fluorescence of live and dead stained cells and did not include EPS. Prior to Ag-NP exposure, the biovolume per image area was 0.015 ± 0.002 μm^3 μm^{-2}, whereas after exposure the biovolume significantly increased to 0.025 ± 0.002 μm^3 μm^{-2} (p=0.019). However, the previously reported range of biomass volumes suggests that biomass variations as these are not surprising. Biomass volume measurements in this study were relatively low compared to *Pseudomonas putida* biofilm grown on 96-well plates in static conditions for 16 hours with biomass volumes ranging 7.04 – 17.56 μm^3 μm^{-2}.[39] Further, when comparing across biofilm studies, the stain type, growth conditions, and image processing software are important variables to consider. Biovolume is a parameter linked to biofilm structure and has been used to identify the effects of changes in environmental conditions, such as dissolved oxygen.[40] The increase in biovolume in this study is a clear display of a structural change after exposure to Ag-NPs.

Biofilm functionality. The capability of biofilm to remove nutrients from wastewater was studied under the exposure of Ag-NP. Typical wastewater constituents were monitored without and with Ag-NPs in the influent after multiple CBR retention times to ensure stability (Table 1). COD reduction percentages in the presence of Ag-NPs showed no significant difference from COD reduction capabilities without Ag-NPs present (p>0.05). Further, no significant difference in pH, sulfate, or ammonia occurred in this continuous flow mesocosm when comparing with and without Ag-NPs present (p>0.05). Without Ag-NPs, the SW showed 122.7 mg L^{-1} of chlorides, whereas with the addition of Ag-NPs in the same SW contained 66.4 mg L-1 of chlorides. This change is expected, as a previous study verified the formation of silver cysteine and histidine, binding with chloride and sulfidic species in wastewater influent.[38] This model biofilm system showed similar resistance to Ag-NPs as RBC biofilms have demonstrated under much higher concentrations of 200 mg L^{-1} with heterotrophic plate counts.[41] As this biofilm community exhibited similar chemical and biological traits to environmental wastewater systems in terms of being able to reduce COD and form a strong biofilm,[42, 43] it will next be applied for understanding sequestration of Ag-NPs from wastewater influent.
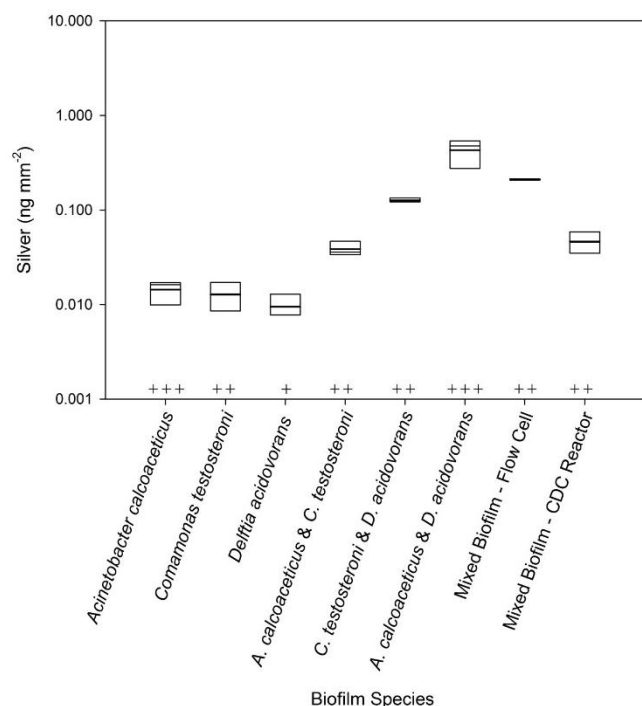
Figure 4. Sorption of Ag-NPs to differently formed model wastewater biofilms are expressed as the 25th and 75th percentile boxplots, with the median represented as an inset bar. Biofilm formation assay results are interpreted as strongly adherent (+++), moderately adherent (++) and weakly adherent (+) as listed above each sample type.

Flow cell exposure tests. The flow cell was inoculated with *C. testosteroni* to first qualitatively test if Ag-NPs adsorb onto/diffuse into biofilms formed on the flow cell coupons. After the biofilm was formed, the flow cell was rinsed with sterile SW and spiked with rhodamine123 protein labeled Ag-NPs (Rh-Ag-NPs) for 10 minutes and rinsed with sterile SW once again. Then, biofilm was stained with Hoescht33358 to identify all cells, and propidium iodide to identify damaged cells (Figure 3). As shown, Rh-Ag-NPs adsorbed to the surface of the biofilm. Image stacks also showed the diffusion of Rh-Ag-NPs into the biofilm structure. Biofilm structure, Ag-NP mobility, and chemical transformation are all important parameters controlling particle diffusion into biofilms. With *Pseudomonas fluorescens*, Ag-NPs have shown to diffuse into biofilms, where the diffusion coefficient changed as the particle size increased.[27] Further, in this study chemical transformation in SW increased the aggregate size, therefore decreased the likeliness that silver species will penetrate deeply into the biofilm.

Biofilm accumulation of silver. With the flow cell system, we then investigated the capacity of each species individually and in combinations to accumulate silver (Figure 4). For each separate experiment, Ag-NP stock was diluted to an estimated 200 ppb. ICP-MS tests showed variations of measured concentrations from 98.8 ppb to 246.4 ppb. The percent of silver retained in

biofilms was calculated by applying a mass balance. For all combinations of species except *A. calcoaceticus* & *D. acidovorans*, the percent of silver accumulated with biofilms compared to measured total silver ranged from 0.27%-1.26%. With the concentration of silver added being exceedingly greater than silver with biofilms, we can assume the influent variations showed minimal influence upon biofilm accumulation. For *A. calcoaceticus* & *D. acidovorans*, the greatest measured accumulation was observed at an influent total silver 105±2.3 ppb, where 7.8% silver sorbed to biofilm. Box plot boundaries show the 25th and 75th percentiles, where the inset line represents the median. The flow cell was operated for single species, dual combinations, and a mixed consortia biofilm. Irrespective of which single species was grown, the silver accumulation per coupon area did not significantly vary ($p > 0.05$). Total silver concentrations for single species biofilms ranged from 0.0078 − 0.017 ng mm^{-2}. The greatest silver accumulation was observed with *A. calcoaceticus* and *D. acidovorans* with a mean of 0.431 ng mm^{-2} per coupon. Dual species combinations which included *D. acidovorans* showed increased silver accumulations compared to the combinations without *D. acidovorans*. *D. acidovorans* is a gold associated microbe and has been used to synthesize gold nanoparticles.[44] Just as *D. acidovorans* overcomes gold toxicity, it shows here that *D. acidovorans* is also tolerant to silver species when associated with other species in a biofilm. In general, as the number of species increased in each experiment, we witnessed an increase in the capacity to accumulate silver. This is somewhat contradictory to the concept that diffusion is more limiting in heterogeneous biofilms compared to a single-species biofilm due to the higher complexity of the matrix.[45] In fact, the increase of complexity in this study shows a trend of increased adsorbed or diffused total silver with the increasing heterogeneity of the biofilm structure. With previous observations that dense biofilms tend to accumulate Ag-NPs to a greater extent than loosely-attached biofilm, we can infer that with increased structural heterogeneity, the biofilm density may also be increasing.[27]

Each species was previously tested in a standard biofilm formation assay. We did not find any correlation between the capacity to form biofilm and the silver accumulated within each biofilm combination. Interestingly, *D. acidovorans* are weakly adherent when grown singly. However in combination with other species the biofilm forming capacity is increased while silver accumulation also showed higher in biofilms containing *D. acidovorans*.

Detachment after silver exposure. The biofilm combination exhibiting the highest accumulation of Ag-NPs, *A. calcoaceticus* and *D. acidovorans*, was chosen for further examination for a potential release of silver as well as biofilm biomass loss through cell detachment. The flow cell accumulation test protocol was repeated; then instead of harvesting the coupons for analysis additional measurements were conducted at two different influent concentrations to monitor both silver release and cell counts within the effluent. After exposure, the flow cell was run with sterilized SW for 10 minutes to flush Ag-NPs from

ARTICLE

bulk liquid. Then as SW was pumped at 2 mL min^{-1}, effluent cell counts and silver concentrations were measured.

low concentration (22 ppb). After flushing Ag-NP with SW from the bulk liquid, silver concentrations did not approach zero after sixty minutes. In fact, effluent total silver averaged 2.6±0.6 ppb for sixty minutes after removing silver from influent. Effluent cell counts ranging from 3.2x10^6 - 1x10^7 cells mL^{-1} before exposure showed no significant difference from cell counts after exposure.

High concentration (105 ppb). At the higher concentration of 105±2.3 ppb Ag-NPs, effluent total silver after flushing averaged 7.9±0.9 ppb for 60 minutes. Effluent cell counts before exposure to this higher concentration significantly decreased from 3x10^7 cell mL^{-1} to a steady cell flow averaging 1.73x10^7 cells mL^{-1} ($p<0.05$, n = 13).

After the 60 minutes of influent flow without silver, biofilm coupons were harvested and analyzed for total silver. At 22 and 105 ppb, total silver remaining adsorbed to biofilm were 0.016 and 0.072 ng mm^{-2}, respectively. Compared to the flow cell accumulation average measurement of 0.431 ng mm^{-2} (Figure 4), there was significant Ag-NP detachment (p=0.04). Previously, silver accumulated in *Pseudomonas fluorescens* biofilm showed to associate more closely with bacterial cells, as opposed to within the EPS.[27] As cells detach, it is reasonable to conclude that silver release was concurrently taking place. We make no correlation to the decrease in detached cells at the high concentration to a decrease in silver concentration within effluent. Overall, even after exposure to Ag-NPs for 30 minutes, it shows here that biofilms can accumulate low concentrations of Ag-NPs in the short term. As this indicates biofilm can become a source from which Ag-NPs can be released, these concentrations are minimal compared to the total silver in the bulk liquid but passed through the system.

Concluding Remarks

This study aimed to answer the question of whether bioaccumulation of ENPs poses hazards to biofilm functions as well as illustrating ENP sequestration effects for multi-component ENP - biofilm systems. The increase in biofilm biovolume indicates a more viscous-like change in the biofilm structure, which is also reinforced by the detection of oxidation stress. Previous studies agree that Ag-NPs at these concentrations do not affect biofilm functional processes, as we showed here for this new mixed model system. Silver accumulation occurred in each type of biofilm within 30 minutes. Biofilm accumulated silver while still protecting the cells within the structure. However, these quantities of silver are minimal considering the total concentration in the wastewater bulk liquid. Longer term exposure would help identify if ENP accumulation in biofilm increases over time.

Conflicts of interest

There are no conflicts to declare.

Acknowledgments

References

1.	T. Schwingle and A. P.C. Simonton, Critical biomass, Public Works, 2009.
2.	M. Wilson, J. Sandino, T. Cote, T. Brueckner, J. Boltz and D. Michelsen, Design and Operational Insights of the World's Largest Integrated Fixed Film Activated Sludge (IFAS) Process for Low Nitrogen Limits, 2012, DOI: info:doi/10.2175/193864712811708248.
3.	J. Wingender, T. R. Neu and H.-C. Flemming, *Microbial extracellular polymeric substances: characterization, structure and function*, Springer Science & Business Media, 2012.
4.	A. F. de Faria, A. C. M. de Moraes and O. L. Alves, in *Nanotoxicology*, eds. N. Durán, S. S. Guterres and O. L. Alves, Springer New York, New York, NY, 2014, pp. 363-405.
5.	C. Walden and W. Zhang, Biofilms Versus Activated Sludge: Considerations in Metal and Metal Oxide Nanoparticle Removal from Wastewater, *Environ Sci Technol*, 2016, **50**, 8417-8431.
6.	K. Ikuma, A. S. Madden, A. W. Decho and B. L. T. Lau, Deposition of nanoparticles onto polysaccharide-coated surfaces: implications for nanoparticle–biofilm interactions, 2014, DOI: 10.1039/C3EN00075C.
7.	Z. Sheng and Y. Liu, Effects of silver nanoparticles on wastewater biofilms, *Water Research*, 2011, **45**, 6039-6050.
8.	O. Choi and Z. Hu, Size Dependent and Reactive Oxygen Species Related Nanosilver Toxicity to Nitrifying Bacteria, *Environ. Sci. Technol.*, 2008, **42**, 4583-4588.
9.	O. Choi, C.-P. Yu, G. Esteban Fernández and Z. Hu, Interactions of nanosilver with Escherichia coli cells in planktonic and biofilm cultures, *Water Research*, 2010, **44**, 6095-6103.
10.	Z. Sheng, J. D. Van Nostrand, J. Zhou and Y. Liu, The effects of silver nanoparticles on intact wastewater biofilms, *Frontiers in Microbiology*, 2015, **6**.
11.	Y. Han, G. Hwang, D. Kim, S. A. Bradford, B. Lee, I. Eom, P. J. Kim, S. Q. Choi and H. Kim, Transport, retention, and long-term release behavior of ZnO nanoparticle aggregates in saturated quartz sand: Role of solution pH and biofilm coating, *Water Research*, 2016, **90**, 247-257.
12.	T. J. Battin, F. v. Kammer, A. Weilhartner, S. Ottofuelling and T. Hofmann, Nanostructured TiO2: transport behavior and effects on aquatic microbial communities under environmental conditions, *Environ. Sci. Technol.*, 2009, **43**, 8098-8104.
13.	J. Fabrega, S. R. Fawcett, J. C. Renshaw and J. R. Lead, Silver Nanoparticle Impact on Bacterial Growth: Effect of pH, Concentration, and Organic Matter, *Environ. Sci. Technol.*, 2009, **43**, 7285-7290.
14.	A. Y. Grün, J. Meier, G. Metreveli, G. E. Schaumann and W. Manz, Sublethal concentrations of silver nanoparticles

This journal is © The Royal Society of Chemistry 2018

Environ. Sci.: Water Research & Tech., 2017, **00**, 1-3 | **7**

affect the mechanical stability of biofilms, *Environmental Science and Pollution Research*, 2016, **23**, 24277-24288.

15. H. Yoo, K.-H. Ahn, H.-J. Lee, K.-H. Lee, Y.-J. Kwak and K.-G. Song, Nitrogen removal from synthetic wastewater by simultaneous nitrification and denitrification (SND) via nitrite in an intermittently-aerated reactor, *Water Research*, 1999, **33**, 145-154.

16. D.-F. Juang, P.-C. Yang, H.-Y. Chou and L.-J. Chiu, Effects of microbial species, organic loading and substrate degradation rate on the power generation capability of microbial fuel cells, *Biotechnology Letters*, 2011, **33**, 2147.

17. M. M. Ballesteros Martín, L. Garrido, J. L. Casas López, O. Sánchez, J. Mas, M. I. Maldonado and J. A. Sánchez Pérez, An analysis of the bacterial community in a membrane bioreactor fed with photo-Fenton pre-treated toxic water, *Journal of Industrial Microbiology & Biotechnology*, 2011, **38**, 1171-1178.

18. D. Djordjevic, M. Wiedmann and L. A. McLandsborough, Microtiter Plate Assay for Assessment of Listeria monocytogenes Biofilm Formation, *Applied and Environmental Microbiology*, 2002, **68**, 2950-2958.

19. S. Andersson, G. Dalhammar, C. J. Land and G. Kuttuva Rajarao, Characterization of extracellular polymeric substances from denitrifying organism Comamonas denitrificans, *Applied Microbiology and Biotechnology*, 2009, **82**, 535-543.

20. G. A. O'Toole, Microtiter Dish Biofilm Formation Assay, *Journal of Visualized Experiments : JoVE*, 2011, DOI: 10.3791/2437.

21. S. Stepanovic, D. Vukovic, I. Dakic, B. Savic and M. Svabic-Vlahovic, A modified microtiter-plate test for quantification of staphylococcal biofilm formation, *Journal of Microbiological Methods*, 2000, **40**, 175-179.

22. L. Mulfinger, S. D. Solomon, M. Bahadory, A. V. Jeyarajasingam, S. A. Rutkowsky and C. Boritz, Synthesis and study of silver nanoparticles, *Journal of chemical education*, 2007, **84**, 322.

23. A. Aranda, L. Sequedo, L. Tolosa, G. Quintas, E. Burello, J. V. Castell and L. Gombau, Dichloro-dihydro-fluorescein diacetate (DCFH-DA) assay: A quantitative method for oxidative stress assessment of nanoparticle-treated cells, *Toxicology in Vitro*, 2013, **27**, 954-963.

24. H. Wang and J. A. Joseph, Quantifying cellular oxidative stress by dichlorofluorescein assay using microplate reader, *Free Radical Biology and Medicine*, 1999, **27**, 612–616.

25. P. Thuptimdang, T. Limpiyakorn, J. McEvoy, B. M. Prü\s s and E. Khan, Effect of silver nanoparticles on Pseudomonas putida biofilms at different stages of maturity, *Journal of Hazardous Materials*, 2015, **290**, 127–133.

26. E. Eruslanov and S. Kusmartsev, in *Advanced protocols in oxidative stress II*, Springer, 2010, pp. 57-72.

27. T.-O. Peulen and K. J. Wilkinson, Diffusion of Nanoparticles in a Biofilm, *Environ. Sci. Technol.*, 2011, **45**, 3367-3373.

28. P. Baumann, Isolation of Acinetobacter from soil and water, *Journal of bacteriology*, 1968, **96**, 39–42.

29. A. M. Maszenan, R. J. Seviour, B. M. Mcdougall and J. A. Soddell, Diversity of isolates of Acinetobacter from activated sludge systems based on their whole cell protein patterns, *Journal of Industrial Microbiology & Biotechnology*, 1997, **18**, 267-271.

30. S. Constantiniu, A. Romaniuc, L. S. Iancu, R. Filimon and I. Taraşi, Cultural and biochemical characteristics of Acinetobacter spp. Strains isolated from hospital units, *J Prevent Med*, 2004, **12**, 35–42.

31. H. F. Retailliau, A. W. Hightower, R. E. Dixon and J. R. Allen, Acinetobacter calcoaceticus: A Nosocomial Pathogen with an Unusual Seasonal Pattern, *The Journal of Infectious Diseases*, 1979, **139**, 371-375.

32. S. V. Gaidhani, R. K. Yeshvekar, U. U. Shedbalkar, J. H. Bellare and B. A. Chopade, Bio-reduction of hexachloroplatinic acid to platinum nanoparticles employing Acinetobacter calcoaceticus, *Process Biochemistry*, 2014, **49**, 2313-2319.

33. R. Singh, P. Wagh, S. Wadhwani, S. Gaidhani, A. Kumbhar, J. Bellare and B. A. Chopade, Synthesis, optimization, and characterization of silver nanoparticles from Acinetobacter calcoaceticus and their enhanced antibacterial activity when combined with antibiotics, *Int J Nanomedicine*, 2013, **8**, 4277–4290.

34. J. Jung and W. Park, Acinetobacter species as model microorganisms in environmental microbiology: current state and perspectives, *Applied Microbiology and Biotechnology*, 2015, **99**, 2533-2548.

35. A. Wen, M. Fegan, C. Hayward, S. Chakraborty and L. I. Sly, Phylogenetic relationships among members of the Comamonadaceae, and description of Delftia acidovorans (den Dooren de Jong 1926 and Tamaoka et al. 1987) gen. nov., comb. nov., *International Journal of Systematic and Evolutionary Microbiology*, 1999, **49**, 567–576.

36. S. Mahmood, K. E. Taylor, T. L. Overman and M. I. McCormick, Acute Infective Endocarditis Caused by Delftia acidovorans, a Rare Pathogen Complicating Intravenous Drug Use, *J. Clin. Microbiol.*, 2012, **50**, 3799-3800.

37. L. Liu, W. Zhu, Z. Cao, B. Xu, G. Wang and M. Luo, High correlation between genotypes and phenotypes of environmental bacteria Comamonas testosteroni strains, *BMC Genomics*, 2015, **16**, 110.

38. G. Brunetti, E. Donner, G. Laera, R. Sekine, K. G. Scheckel, M. Khaksar, K. Vasilev, G. De Mastro and E. Lombi, Fate of zinc and silver engineered nanoparticles in sewerage networks, *Water Research*, 2015, **77**, 72-84.

39. P. Thuptimdang, T. Limpiyakorn and E. Khan, Dependence of toxicity of silver nanoparticles on Pseudomonas putida biofilm structure, *Chemosphere*, 2017, **188**, 199-207.

40. M.-A. Yun, K.-M. Yeon, J.-S. Park, C.-H. Lee, J. Chun and D. J. Lim, Characterization of biofilm structure and its effect on membrane permeability in MBR for dye wastewater treatment, *Water Research*, 2006, **40**, 45-52.

41. Z. Sheng and Y. Liu, Effects of silver nanoparticles on wastewater biofilms, *Water Research*, 2011, **45**, 6039-6050.

42. T. Eighmy, D. Maratea and P. Bishop, Electron microscopic examination of wastewater biofilm formation and structural components, *Applied and environmental microbiology*, 1983, **45**, 1921-1931.

43. A. A. U. de Souza, H. L. Brandao, I. M. Zamporlini, H. M. Soares and S. M. d. A. G. Ulson, Application of a fluidized bed bioreactor for cod reduction in textile industry effluents, *Resources, Conservation and Recycling*, 2008, **52**, 511-521.

44. C. Ganesh Kumar, Y. Poornachandra and S. K. Mamidyala, Green synthesis of bacterial gold nanoparticles conjugated

8 | *Environ. Sci: Water Research & Tech.*, 2012, **00**, 1-3

This journal is © The Royal Society of Chemistry 2018

to resveratrol as delivery vehicles, *Colloids and Surfaces B: Biointerfaces*, 2014, **123**, 311-317.

45. E. Guiot, P. Georges, A. Brun, M. P. Fontaine-Aupart, M. N. Bellon-Fontaine and R. Briandet, Heterogeneity of Diffusion Inside Microbial Biofilms Determined by Fluorescence Correlation Spectroscopy Under Two-photon Excitation, *Photochemistry and Photobiology*, 2002, **75**, 570-578.

This journal is © The Royal Society of Chemistry 2018

Environ. Sci.: Water Research & Tech., 2017, **00**, 1-3 | **9**